mathematics

MDPI

Article

LMPSeizNet: A Lightweight Multiscale Pyramid Convolutional Neural Network for Epileptic Seizure Detection on EEG Brain Signals

Arwa Alsaadan, Mai Alzamel * and Muhammad Hussain

Department of Computer Science, College of Computer and Information Sciences, King Saud University, Riyadh 11451, Saudi Arabia; 442202742@student.ksu.edu.sa (A.A.); mhussain@ksu.edu.sa (M.H.)
* Correspondence: malzamel@ksu.edu.sa

Abstract: Epilepsy is a chronic disease and one of the most common neurological disorders worldwide. Electroencephalogram (EEG) signals are widely used to detect epileptic seizures, which provide specialists with essential information about the brain's functioning. However, manual screening of EEG signals is laborious, time-consuming, and subjective. The rapid detection of epilepsy seizures is important to reduce the risk of seizure-related implications. The existing automatic machine learning techniques based on deep learning techniques are characterized by automatic extraction and selection of the features, leading to better performance and increasing the robustness of the systems. These methods do not consider the multiscale nature of EEG signals, eventually resulting in poor sensitivity. In addition, the complexity of deep models is relatively high, leading to overfitting issues. To overcome these problems, we proposed an efficient and lightweight multiscale convolutional neural network model (LMPSeizNet), which performs multiscale temporal and spatial analysis of an EEG trial to learn discriminative features relevant to epileptic seizure detection. To evaluate the proposed method, we employed 10-fold cross-validation and three evaluation metrics: accuracy, sensitivity, and specificity. The method achieved an accuracy of 97.42%, a sensitivity of 99.33%, and a specificity of 96.51% for inter-ictal and ictal classes outperforming the state-of-the-art methods. The analysis of the features and the decision-making of the method shows that it learns the features that clearly discriminate the two classes. It will serve as a useful tool for helping neurologists and epilepsy patients.

Keywords: epileptic seizures detection; EEG signals; deep learning; CNN model; neurological disorders

MSC: 68T07

check for updates

Citation: Alsaadan, A.; Alzamel, M.; Hussain, M. LMPSeizNet: A Lightweight Multiscale Pyramid Convolutional Neural Network for Epileptic Seizure Detection on EEG Brain Signals. *Mathematics* **2024**, *12*, 3648. https://doi.org/10.3390/math12233648

Academic Editors: Miguel Enrique Iglesias Martínez and Pedro José Fernández de Córdoba Castellá

Received: 1 October 2024
Revised: 14 November 2024
Accepted: 16 November 2024
Published: 21 November 2024

Copyright: © 2024 by the authors. Licensee MDPI, Basel, Switzerland. This article is an open access article distributed under the terms and conditions of the Creative Commons Attribution (CC BY) license (https://creativecommons.org/licenses/by/4.0/).

1. Introduction

Epilepsy is a chronic disease and one of the most common neurological disorders around the world, and it is characterized by sudden recurrent seizures [1]. The human brain consists of several neurons, and sometimes a severe disturbance of these neurons occurs, causing a seizure [2]. The disturbance of neurons results from many different reasons such as genetics or structural change in the brain and others. More than 60 million people in the world have been affected by epileptic seizures of various kinds [3]. Epileptic seizures may lead to temporary confusion, sudden loss of consciousness or awareness, uncontrollable jerking and shaking, and so on [4], which can cause severe injury or loss of life resulting from falls and accidents. In addition, it affects the patient's psychological, occupational, and social aspects. Therefore, rapid and accurate detection of epileptic seizures will help to minimize financial and living costs, i.e., improving the patient's quality of life [5].

There are different screening techniques to detect epileptic seizures, such as magnetic resonance imaging (MRI) [6], electroencephalogram (EEG) [7], and magnetoencephalography (MEG) [8]. The observation of brain activity signals using the EEG technique is the most

common method for detecting epileptic seizures [9]. Recording and observing the electroencephalogram (EEG) signal is one of the primary tools for detecting epileptic seizures [10]. It is a technique that includes placing many electrodes on a patient's scalp [11] to capture the electrical activities of neurons as an EEG signal [12]. These complex biomedical one-dimensional signals are difficult to visually observe [13] because of the difficulty of analyzing long-term EEG recordings, especially if the observation is multichannel [10]. This necessitated the need for automatic machine learning-based methods for epileptic seizures.

Recently, due to the marvelous achievements of deep learning, it has been employed in designing methods for epileptic seizure detection [1–3]. Several studies have shown that the CNN architecture is the most suitable for EEG signal representation learning because it has the advantage of preserving the structural and configurational information in the original data [4–6]. However, the way the CNN architecture has been used to develop methods for the automatic screening of EEG signals has certain limitations and needs further improvement. Most of the CNN architectures employed in recent studies are composed of stacked convolutional layers, meaning the extracting features process is performed sequentially [3,14]. Cimr et al. [14] introduced a lightweight CNN model where eight learnable layers are stacked in sequential order. Though the model proposed by Cimr et al. [14] is lightweight, it does not take into account the multiscale information of EEG signals. Most of the sequential CNN models require a large number of training samples because of the enormous number of learnable parameters [3,15], while annotated epileptic seizures EEG data are limited [7]. It was shown by Ko et al. [16] that a multiscale neural network (MSNN) extracts features at multiple frequency/time ranges, which better reflect the multi-frequency properties in EEG signals. There are no significant studies that leverage the multiscale nature of EEG signals. Most of the existing CNN architectures stack convolutional layers so that the width of the network (the number of filters in convolutional layers) increases with increasing depth; this drastically increases the number of learnable parameters, leading to overfitting. Ihsan et al. [17] showed that the pyramid architecture design, where a CNN model's width decreases with increasing depth, significantly reduces its complexity, avoiding overfitting problems when the available annotated data are limited.

Inspired by the superior performance of the multiscale neural network and the parameter reduction efficiency of pyramid architecture, we design a new lightweight multiscale convolutional neural network, namely, LMPSeizNet, to detect the epileptic patient's state, whether he/she is in an inter-ictal or ictal state. LMPSeizNet blends the design idea of encoding multiscale information similar to MSNN [16] and the concept of pyramid architecture to keep its architecture simple, efficient, and expressive to avoid overfitting and enhance its generalization. The main contributions of this work are as follows:

- We proposed a lightweight multiscale CNN model, named LMPSeizNet, for epileptic seizure detection. It is very efficient and expressive, i.e., it efficiently analyzes the temporal (along the time dimension) and spatial (along the channel dimension) to encode spectral information using temporal filters of various receptive fields to learn the multiscale discriminative features from EEG signals relevant to epileptic seizure detection. Moreover, as it is based on the pyramid architecture design, it is lightweight, i.e., the number of learnable parameters is small, and a limited number of annotated EEG trials is enough to train it to avoid overfitting.
- We implemented and thoroughly analyzed the performance of LMPSeizNet on benchmark datasets. The results and analysis indicate that it has comparable or better performance than similar state-of-the-art methods while keeping its parameter complexity low, enhancing its generalization despite limited annotated EEG trials.

The rest of this paper is organized as follows. Section 2 presents a review of the state-of-the-art methods for epileptic seizure detection. Section 3 gives the details of the proposed method. Section 4 describes the experimental setup and evaluation protocol. Section 5 presents the details of the experiments conducted to validate the performance of the proposed method. Section 6 demonstrates the results achieved, and Section 7 provides

a discussion and a comparison with the state-of-the-art results. Finally, Section 8 provides the conclusion.

2. Literature Review

Many researchers have addressed the problem of epilepsy detection using EEG brain signals, and different methods have been proposed. These methods can be classified into two main categories: hand engineering features-based and deep learning-based methods. Different approaches have been used to extract hand-engineered features from EEG signals for epilepsy detection [10,18–21]. Though these methods achieved satisfactory results, they have some limitations; their time complexity is high [20], they are limited to certain small-size datasets and do not generalize to the other datasets [18], and they require increasing training time and memory usage to improve the accuracy of the models [22]. In contrast, the deep learning approaches are more robust compared to hand-engineered feature-based approaches and provide better classification performance. Consequently, we present below an overview of the state of the art using hand engineering and deep learning-based methods for epileptic seizure detection.

Some methods have been proposed based on the traditional machine learning approach, where hand-engineered feature extraction techniques are used to extract discriminative information and classification methods for detection [23–25]. Rafiamma et al. [26] developed an algorithm using hand engineering approaches for automatic epileptic seizure detection. This method is based on discrete wavelet transform and the cluster-based nearest neighbor algorithm. This method provides low classification performance between seizure and normal EEG signals, and its complexity is high. Zarei [27] introduced a method based on features extracted from EEG signals using discrete wavelet transform, orthogonal matching pursuit, and entropy. Li et al. [25] used nonlinear mode decomposition and KNN for their method of epileptic seizure detection. Zabihi et al. [24] proposed a method using nonlinear dynamics and nullclines for patient-specific epileptic seizure detection.

Different deep learning-based approaches used for epileptic seizure detection are 1DCNN [12,28,29], 1DCNN and 2DCNN [30,31], CNN and LSTM [4,32], and others [33,34]. Wang et al. [12] developed a stacked one-dimensional convolutional neural network (1DCNN) model and used the random selection and data augmentation (RS-DA) strategy for training. Gupta et al. [28] introduced a model to maintain the true nature of EEG signals by using 1DCNN to assist neurosurgeons in easily defining the affected part of the brain. Jia et al. [29] introduced the variable weight convolutional neural networks (VWCNNs) technique, which uses dynamic weights instead of static weights in the convolutional layers and fully connected layers to mitigate the limitations of generalization ability and classification performance resulting from static weights.

Wang et al. [31] proposed a method based on 1DCNN and 2DCNN to detect seizures from EEG signals. The complexity of the learnable parameters of this method is very high, leading to overfittings. Xu et al. [4] introduced a 1D CNN-LSTM model for epileptic detection. Firstly, EEG trials are preprocessed and normalized, and then features are extracted using the CNN model. After that, temporal features are extracted by LSTM layers, and the classification is performed. Liu et al. [32] introduced a novel deep CNN-LSTM structure for detecting seizures and tumors and determining the status of the two eyes (closed or open). The proposed method proved capable of detecting a seizure using a short EEG signal segment (1 s).

Some methods used architectures like autoencoder [33] and generalized convolutional prototype learning (GCPL) [34]. Shoka et al. [35] integrated a CNN model with autoencoders (A.E.s) to reduce wrong warnings during epileptic seizure detection. The authors noticed that the classification performance of this method is similar to that of a CNN model but with a decrease in the average false positive rate. Abdelhameed et al. [36] proposed a new method based on the automatic feature learning capabilities of a two-dimensional deep convolution autoencoder in addition to a neural network-based classifier. The study

shows high performance in seizure classification; however, the proposed model has a very high parameter complexity.

José et al. [37] introduced a new method for epileptic seizure classification based on a deep belief network (DBN). The performance of this method is low compared to the state-of-art methods. The reason is that the CNN- and RNN-based techniques outperform perform the DBN-based methods. Mekruksavanich and Jitpattanakul [38] proposed a deep model, ResNet-BiGRU-ECA, composed of three types of layers: convolutional layers, BiGRU layers, and channel attention layers. The proposed method was evaluated on the ESRD dataset using 5-fold cross-validation. Despite the good reported performance, the model has high parameter complexity, which leads to overfitting. Cimr et al. [14] developed a deep CNN model consisting of learnable layers; it performs well and has low parameter complexity. However, the model does not take into account the multiscale information of EGG signals. Abdulwahhab et al. [15] introduced a hybrid deep model consisting of CNN and RNN blocks. The RNN block takes raw EEG signals as input. In parallel, the signal is transformed into spectrogram and scalogram images and passed to the CNN block. Though it shows good classification performance, it is very complex and has high parameter complexity.

Some deep learning-based techniques first convert EEG signals to an image and use highly complex CNN architectures. Lyu et al. [34] presented a method based on generalized convolutional prototype learning (GCPL). The authors used VGG16 for feature evaluation and GCPL for classification. It integrates a CNN model and prototype learning. GCPL assigns EEG samples to the prototype's nearby areas in the feature space. Notably, the complexity of VGG16 is very high. Tripath et al. [39] proposed a new method that first converts an EGG trial into 2D images using superset transform (SLT) to be passed to VGG-19 for seizure classification. This method has a very high parameter complexity due to converting EEG singles to 2D images and using VGG-19.

In general, deep learning-based methods show better performance compared to hand-engineered features-based methods, and the dominant deep architecture is a CNN, which has shown better performance. However, the designs of CNN architectures used in the existing methods for the automatic screening of EEG signals for epileptic seizure detection have certain limitations. Most CNN architectures stack convolutional layers and extract features sequentially, ignoring the fact that features in an EEG signal exist at multiple scales. In addition, these architectures have an enormous number of learnable parameters requiring a huge amount of data for their training, while the annotated epileptic seizures EEG data are limited.

3. Propped Method

In this section, we first present the problem specification and formulation, and then we present the details of the proposed method for seizure detection LMPSeizNet.

3.1. Problem Formulation

The problem is to detect through an epoch of the EEG signal of an epileptic patient whether he/she is in an inter-ictal or ictal state. In machine learning, this can be formulated as a classification problem, where the given epoch of an EEG signal is classified into one of two classes, i.e., inter-ictal or ictal, as shown in Figure 1.

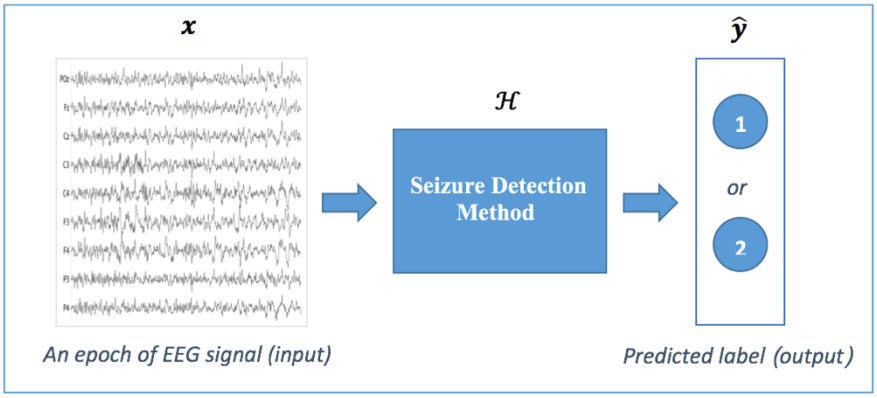

Figure 1. Seizure detection problem specification, where 1 and 2 are labels that stand for inter-ictal and ictal classes. Here, $\boldsymbol{x}$ is an EEG signal epoch to be passed to a seizure detection method ($\mathcal{H}$) for its classification.

The EEG signal taken from an epileptic patient consists of two dimensions: spatial and temporal. The spatial dimension represents different locations on the scalp, while the temporal dimension represents the time points that determine the change in the EEG signal over time. The EEG signal is segmented into epochs (instances) with a fixed temporal window. Each epoch $\boldsymbol{x}$ consists of C channels and T time points; it is represented as a matrix:

$$\boldsymbol{x} = \begin{pmatrix} x_{1,1} & x_{1,2} & \cdots & x_{1,T} \\ x_{2,1} & x_{2,2} & \cdots & x_{2,T} \\ \vdots & \vdots & \ddots & \vdots \\ x_{C,1} & x_{C,2} & \cdots & x_{C,T} \end{pmatrix}, \quad \text{i.e.,} \quad x \in R^{C \times T}, \tag{1}$$

In this matrix, the rows represent the spatial dimension, and the columns represent the temporal dimension. It indicates that $\boldsymbol{x}$ belongs to the space of EEG epochs $R^{C \times T}$, i.e., $\boldsymbol{x} \in R^{C \times T}$. Let $Y = \{1, 2\}$ be the set of labels, where labels 1 and 2 represent inter-ictal and ictal (seizure) classes, respectively. Formally, to predict the state of an epoch $\boldsymbol{x}$ as inter-ictal, or ictal, we need to design a mapping that takes $\boldsymbol{x}$ as input and yields $\hat{y}$ as output, where $\hat{y} \in Y$ is the predicted label of $\boldsymbol{x}$. This means that we need to design the mapping $\mathcal{H}(\boldsymbol{x}, \theta) : R^{C \times T} \rightarrow Y$ so that $\mathcal{H}(\boldsymbol{x}, \theta) = \hat{y}$, where θ represent the parameters of mapping $\mathcal{H}$. The main problem is to design $\mathcal{H}$ so that it can accurately detect the actual label of any input epoch. Motivated by the outstanding performance of deep learning-based techniques [16], we design $\mathcal{H}$ as a lightweight multiscale pyramid convolutional neural network model for seizure detection (LMPSeizNet).

3.2. Lightweight Multiscale Pyramid Convolutional Neural Network (LMPSeizNet)

A close look at the EEG epoch shown in Figure 2 reveals that each channel is composed of multiple scales/frequencies along the temporal dimension. This indicates that extracting multiscale temporal features is the best approach to represent an EEG signal. Further, the signal varies across channels along the spatial dimension at each time point, and the spatial variations are correlated; this observation suggests extracting multiscale spatial patterns along the spatial dimension. Motivated by these characteristics of EEG signals and the deep multiscale neural network proposed by Ko et al. [16], we propose an end-to-end lightweight multiscale pyramid convolutional neural network (LMPSeizNet) for modeling $\mathcal{H}$. LMPSeizNet extracts features at multiple frequencies/scales along temporal dimensions and encodes the relationships among channels to reflect the multiscale properties of EEG signals. It is composed of three mappings: the multiscale-temporal feature representation (ϕ^1), the spatial feature representation (ϕ^2), and the classifier (ϕ^3), as illustrated in Figure 3. In view of this, the model $\mathcal{H}$ is composed of three mappings as follows:

$$\mathcal{H}(x; \theta) = \phi^1 \circ \phi^2 \circ \phi^3(x), \tag{2}$$

where θ represents the learnable parameters of ϕ^1, ϕ^2, and ϕ^3. The details of each mapping are described in the following subsections.

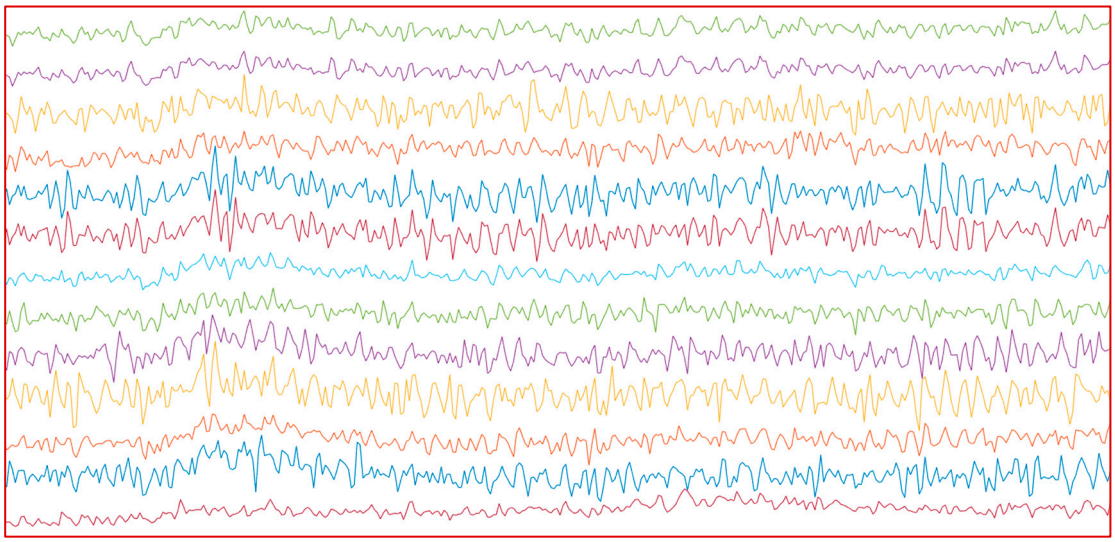

Figure 2. An example EEG epoch showing that each of its channels is the superposition of several frequencies along the time dimension, and it is necessary to analyze it using multiscale convolution. Each EGG channel represent in different color.

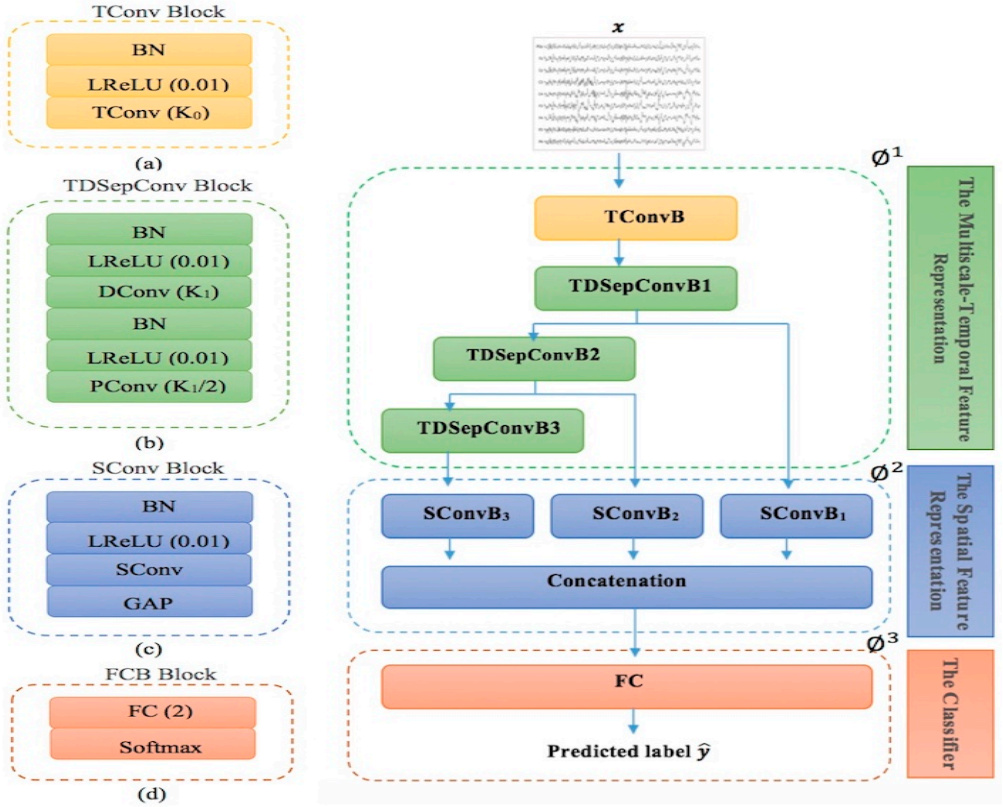

Figure 3. The architecture of LMPSeizNet; it takes an EEG trial as input and processes it using three main modules, defining the mappings of ϕ^1, ϕ^2, and ϕ^3, and yields the predicted label $\hat{y}$. Where (**a**) is the first temporal convolution block, (**b**) is temporal separable convolutional block, (**c**) is spatial convolutional block, (**d**) is the classifier.

3.2.1. The Multiscale Temporal Feature Representation

The mapping ϕ^1 analyses the input EEG epoch x using multiple temporal filters and extracts multiscale temporal features. For this purpose, one temporal convolution block and three temporal depthwise separable convolution blocks are employed to extract multiscale temporal features in sequence.

The first temporal convolution (TConvB) block uses K_0 one-dimensional (1D) temporal filters of size $K_0 = 1 \times (f_s/2) \times 1$, where f_s denotes the sampling rate; it extracts frequencies of 4 Hz and above. It uses a leaky rectified linear unit (LReLU) activation function to overcome ReLU's vanishing gradient issues. It takes an EEG epoch $x \in R^{C \times T}$ as input and yields the activation $\mathcal{F}_0 \in R^{C \times T \times K_0}$, a feature map consisting of K_0 features of size $C \times T$, i.e., $\mathcal{F}_0 = \left[f_0^1, f_0^2, \ldots, f_0^{K_0}\right]$, where $f_0^i \in R^{C \times T}$ is a feature learned by the ith filter. This block learns K_0 different spectral features with frequencies 4 Hz and above from the input EEG epoch.

The three-temporal depth-wise separable convolution (TDSepConvB) blocks extract multiscale temporal features sequentially; the specification of a TDSepConvB block is shown in Figure 3; it consists of six layers. Batch normalization layers are used to overcome the vanishing gradient problem during backpropagation and to speed up the convergence while training the network. The activation layers LReLU introduce the non-linearity in the network and speed up the convergence, avoiding the gradient vanishing problem. Each TDSepConvB block involves two main learnable layers: a depthwise convolution (DConv) and a pointwise convolution (PConv). The DConv layer of the first TDSepConvB1 block takes the output $\mathcal{F}_0 = \left[f_0^1, f_0^2, \ldots, f_0^{K_0}\right]$ of TConvB block as input and uses as many filters as there are features in the input feature map $\mathcal{F}_0$, i.e., K_0 1D filters of size $k_1^1 = 1 \times T_1$, which means that one independent filter is learned for each input feature to learn a more expressive feature. It yields an activation $\mathcal{F}_1^1 = \left[g_1^1, g_1^2, \ldots, g_1^{K_0}\right]$. The DConv does not take into account the interdependencies between features g_0^i, i = 1, 2, …, K_0; this is dealt with by the PConv layer, which takes $\mathcal{F}_1^1$ as input and uses pointwise convolution with K_1 1D filters of size $k_1^2 = 1 \times 1$ to generate a richer feature map $\mathcal{F}_1^2 = \left[f_1^1, f_1^2, \ldots, f_1^{K_1}\right] \in R^{C \times T \times K_1}$. Note that $K_1 < K_0$, which indicates that the PConv layer generates discriminative features by reducing the dimension of the input space and avoiding the curse of the dimensionality problem.

Similarly, the TDSepConvB2 and TDSepConvB3 blocks take $\mathcal{F}_1^2 \in R^{C \times T \times K_1}$ and $\mathcal{F}_2^2 \in R^{C \times T \times K_2}$ as inputs, respectively, use K_i $(i = 1, 2)$1D filters of size $k_j^1 = 1 \times T_j$ $(j = 2, 3)$ for DConv layers and K_j $(j = 2, 3)$ filters of size $k_j^2 = 1 \times 1$ for PConv layers, and give rise to the feature maps $\mathcal{F}_2^2 \in R^{C \times T \times K_2}$ and $\mathcal{F}_3^2 \in R^{C \times T \times K_3}$, respectively.

Note that we use the pyramid approach [17] to specify the numbers K_j $(j = 1, 2, 3)$ in TDSepConvB blocks such that $K_1 > K_2 > K_3$, which helps to extract larger numbers of low-level features and small numbers of higher-level discriminative features hierarchically. An advantage of this approach is the significant reduction in the number of unnecessary learnable parameters, which helps reduce the chances of overfitting because the available annotated data for training the network are limited. Additionally, the filter sizes $k_j^1 (j = 1, 2, 3)$ in TDSepConvB blocks are chosen such that $T_1 > T_2 > T_3$; this choice helps to extract multiscale discriminative features at different levels of the hierarchy. Empirically, we found that the best values for these hyperparameters are $K_0 = 64$, $K_1 = 32$, $K_2 = 16$, $K_3 = 8$, $T_1 = 32$, $T_2 = 16$, $T_3 = 8$. The detailed specification of these blocks is shown in Table 1.

Table 1. The specification of the architecture of LMPSeizNet, together with the parameter complexity of each block. The stride for each of TConvB and TDSepConvB is set to 1.

Mapping	Block	Input	Output	Learnable Parameters
ϕ^1	TConvB $K_0 = 64,\ T_0 = fs/2$	$3 \times 512 \times 1$	$3 \times 385 \times 64$	8256
	TDSepConvB1 $K_1 = 32,\ T_1 = 32$	$3 \times 512 \times 64$	$3 \times 354 \times 32$	4192
	TDSepConvB2 $K_2 = 16,\ T_2 = 16$	$3 \times 354 \times 32$	$3 \times 339 \times 16$	1072
	TDSepConvB3 $K_3 = 8,\ T_3 = 8$	$3 \times 339 \times 16$	$3 \times 332 \times 8$	280
ϕ^2	SConvB1 $K_4 = 32,\ k_4 = [C, 1, K_1]$	$3 \times 354 \times 32$	$1 \times 1 \times 32$	3104
	SConvB2 $K_5 = 16,\ k_5 = [C, 1, K_2]$	$3 \times 339 \times 16$	$1 \times 1 \times 16$	784
	SConvB3 $K_6 = 8,\ k_5 = [C, 1, K_3]$	$3 \times 332 \times 8$	$1 \times 1 \times 8$	224
ϕ^3	Concatenation	$(1 \times 1 \times 32)$, $(1 \times 1 \times 16)$, $(1 \times 1 \times 8)$	$1 \times 1 \times 56$	
	FCB	1×56	2	112
		Total		18,024

The output of the mapping ϕ^1 is $[\mathcal{F}_1^2,\ \mathcal{F}_2^2,\ \mathcal{F}_3^2]$, i.e.,

$$\left[\mathcal{F}_1^2,\ \mathcal{F}_2^2,\ \mathcal{F}_3^2\right] = \phi^1(x; \theta_1), \tag{3}$$

which is passed to the next module to extract the most discriminative features; here, θ_1 are the learnable parameters of ϕ^1.

3.2.2. The Spatial Feature Representation

The mapping ϕ^1 analyses the input EEG epoch $\boldsymbol{x}$ along the temporal dimension and ignores the spatial relationships of the features. The mapping ϕ^2 overcomes this limitation and works out the spatial relationships between multiscale temporal features. It consists of three spatial convolutional (SConvB) blocks, which take multiscale temporal feature maps as input and yield multiscale spatial patterns.

Each SConvB consists of four layers, as shown in Figure 3. The SConvB1 block takes $\mathcal{F}_1^2 \in R^{C \times T \times K_1}$ as an input, processes it with the B.N. layer, activation LReLU, spatial convolution (SConv) layer, and global average pooling (GAP) layer and extracts the feature vector $v_1 \in R^{1 \times 1 \times K_4}$. The SConv layer uses K_4 1D spatial filters of sizes $k_4 = C \times 1$ and learns feature maps of dimension $1 \times T \times K_4$, which is further reduced to the dimension $1 \times 1 \times K_4$ with the GAP layer. Similarly, the feature maps $\mathcal{F}_2^2 \in R^{C \times T \times K_2}$ and $\mathcal{F}_3^2 \in R^{C \times T \times K_3}$ are passed to the SConvB2 and SConvB3 blocks, respectively, which use K_5 and K_6 1D spatial filters of sizes $k_{j+3} = C \times 1,\ j = 2,\ 3$, and learn the feature vectors $v_2 \in R^{1 \times 1 \times K_5}$ and $v_3 \in R^{1 \times 1 \times K_6}$, respectively. The multiscale temporo-spatial features v_1, v_2, v_3 are concatenated to generate a feature vector $v \in R^{3K_4}$, which is passed to the classification module. The above discussion indicates that the mapping ϕ^2 takes $\mathcal{F}_i^2 \in R^{C \times T \times K_i},\ i = 1,\ 2,\ 3$, and extract the feature vector $v \in R^{3K_4}$, i.e.,

$$v = \phi^2\left(\mathcal{F}_1^2,\ \mathcal{F}_2^2,\ \mathcal{F}_3^2;\ \theta_2\right), \tag{4}$$

where θ_2 are the learnable parameters of ϕ^2. The outputs of TDSepConvB1 and TDSepConvB2 are passed directly to SConvB1 and SConvB2 through shortcut connections to generate multi-scale features. These shortcuts make the flow of gradients easy during the backpropagation and help to overcome the training difficulties due to the gradient vanishing problem.

3.2.3. The Classifier

The mappings ϕ^1 and ϕ^2 form the feature extractor, which analyzes the input EEG epoch x and extracts multiscale temporo-spatial features $v \in R^{3K_4}$. These features are passed to the classifier ϕ^3, which calculates the posterior probability of each class using an F.C. layer and a softmax layer, i.e.,

$$p = \phi^3(v;\ \theta_3), \tag{5}$$

where p is the vector of posterior probabilities and θ_3 represents the weights and biases of the F.C. layer. The most probable class, i.e., the class with the highest posterior probability, is the predicted class of the input EEG epoch x. The model $\mathcal{H}(x;\theta)$ is learned end-to-end so that the loss is minimal, i.e.,

$$\hat{\theta} = \min_{\theta} \sum l(\ \mathcal{H}(x;\theta),\ y), \tag{6}$$

where $l(.,\ .)$ is the loss function, and $\mathcal{H}(\boldsymbol{x};\theta)$ and y are the predicted and actual labels of $\boldsymbol{x}$. Here, θ represents the learnable parameters of ϕ^1, ϕ^2, and ϕ^3, i.e., $\theta = \{\theta_1,\ \theta_2,\ \theta_3\}$.

Please note that LMPSeizNet is lightweight; it involves only 18,024 learnable parameters, whereas the MSNN model [16] involves a large number of trainable parameters, which is 202,576. This means that LMPSeizNet can be trained using the limited annotated data available, avoiding overfitting issues.

4. Evaluation Protocol

In this section, we first present the description of the dataset and how it was prepared for conducting experiments to validate the performance of LMPSeizNet. Then, we describe the details of the framework that we used to perform experiments. Additionally, we highlight the training procedure for LMPSeizNet. Finally, we state the evaluation metrics used to measure the performance of LMPSeizNet. All experiments were performed on a PC equipped with 128 GB of RAM and an NVIDIA Quadro RTX 6000 GPU. The model was implemented using the MATLAB Deep Learning Toolbox R2022b.

4.1. Dataset and Data Preparation

To implement our method, we used the CHB-MIT dataset, collected at the Children's Hospital Boston, consisting of EEG recordings of children with epilepsy [40]. The database is publicly available [41]. More details about the dataset are provided below: The CHB-MIT database has been used in recent work for epileptic seizure classification [16]. This database contains EEG signals of 24 subjects sampled at 256 Hz. EEG signals were recorded using 23 electrodes (24 or 26 in a few cases), namely, FP1-F7, F7-T7, T7-P7, P7-O1, FP1-F3, F3-C3, C3-P3, P3-O1, FP2-F4, F4-C4, C4-P4, P4-O2, FP2-F8, F8-T8, T8-P8, P8-O2, FZ-CZ, CZ-PZ, P7-T7, T7-FT9, FT9-FT10, FT10-T8, and T8-P8 [42], using the international 10–20 placement system. Some subjects have ictal periods of less than 6 s. However, according to the opinion of electroencephalographers, a neurological disorder depicted in EEG signals can be considered a seizure if it persists and evolves for more than six seconds [43]. As such, to validate our method, we selected the EEG signals of 11 subjects (chb01, chb02, chb03, chb07, chb10, chb17, chb18, chb19, chb20, chb21, and chb22) who had seizures for a duration of at least 6–10 s. Further, though the EEG signals were recorded using the international 10–20 placement system, we found that all files associated with three subjects (i.e., chb18, chb20, and chb22) have different channel montages from the rest. Accordingly, we excluded these three subjects also and finally used the data from eight subjects. Also, among 23 channels, FP1-F3, F4-C4, FP2-F8, CZ-PZ, and T8-P8 include a large number of not-a-number (NaN) entries, so these channels were excluded.

We worked on creating trials for the dataset of three classes: inter-ictal, pre-ictal, and ictal. First, we loaded the data for each person as described in Section 4.1. Then, we read the EEG in .edf files and the seizure-labeled files in the .txt file that contains the seizure time. After that, we divided the EEG signal into three segments: inter-ictal, pre-ictal, and ictal. The pre-ictal state is 10 min before the seizure starts [44], the ictal state time is specified in the .txt file for each EEG, and the inter-ictal state represents the residual of the EEG signal. Afterward, we segmented the EEG signal corresponding to each state into trials. Finally, we saved all inter-ictal trials, all pre-ictal trials, and all ictal trials in .mat file for each subject.

4.2. Evaluation Procedure and Metrics

To validate the performance of LMPSeizNet, we used the subject-independent evaluation with 10-fold cross-validation, an approach adopted in state-of-the-art methods. In this approach, the dataset from all subjects is divided into ten folds, and the same experiment is repeated ten times for each fold in such a way that eight folds are used for training, one fold is used for validation, and one fold is used for testing. This process ensures that every time, the model is trained on different datasets and tested on different sets, which helps to assess the robustness and generalization of the model. The experiments were conducted on the Google Cloud Platform. The model was trained using the Adaptive Moment Estimation (ADAM) optimizer. The learning rate used for training was 0.01.

To measure the performance of LMPSeizNet, we used three performance measurements: accuracy, sensitivity, and specificity. Accuracy represents the ratio of all correctly classified EEG epochs among all tested subjects. Sensitivity is defined as the ratio of correctly classified ictal EEG epochs (T.P.) to the total number of correctly classified and misclassified ictal EEG epochs. Specificity is defined as the ratio of correctly classified inter-ictal EEG epochs (T.P.) to the total number of correctly classified and misclassified inter-ictal EEG epochs. The accuracy, sensitivity, and specificity are defined formally in Equations (7)–(9), respectively. The effectiveness of classification methods depends on providing high rates of these metrics.

$$Accuracy = TP + TN/(TP + TN + FP + FN), \tag{7}$$

$$Sensitivity = TP/(TP + FN), \tag{8}$$

$$Sepecificity = TN/(TN + FP) \tag{9}$$

5. Ablation Study

In this section, we present the details of different experiments that were conducted to find the best configuration of LMPSeizNet and tune the hyperparameters. Also, we discuss the results obtained in all these experiments.

5.1. Configuration of LMPSeizNet

We performed several experiments with two classes (inter-ictal and ictal) to find the best configuration of LMPSeizNet that gives the best performance. We used experiments with two classes (inter-ictal and ictal) to fine-tune the hyperparameters, including filter size, number of filters, the size of strides, and the number of channels in each epoch (EEG trial).

5.1.1. The Impact of Pyramid Architecture

In this experiment, we focused on finding the LMPSeizNet model's best architecture, which gives the best performance and involves less complexity. We conducted this experiment using EEG trials composed of three channels: {FP1-F7, F7-T7, T7-P7}, and the number of training epochs for the optimizer for training the model was set equal to five. As shown in Table 2, we fixed the number of filter sizes and changed the number of filters according to the pyramid design approach [36]; specifically, we decreased the number of filters rather than increasing them. The results in Table 3 show that the pyramid design approach provides better accuracy, sensitivity, and specificity results, which are 86.94%, 88.52%, and 85.36%, respectively. In contrast, the traditional approach gives accuracy,

sensitivity, and specificity of 82.78%, 84.53%, and 81.03%, respectively. In the following experiments, we fix the pyramid architecture.

Table 2. Results showing the comparison of the two design approaches, pyramid and traditional, with the channels {FP1-F7, F7-T7, T7-P7}.

Approach	Filter Size	#Filters	Acc (%)	Sen (%)	Spe (%)
	T_0, T_1,T_2, T_3	K_0, K_1 ,K_2, K_3,K_4 ,K_5, K_6			
Pyramid	128, 64, 32,16	64, 32, 16, 8, 32, 16, 8	86.94	88.52	85.36
Traditional	128, 64, 32, 16	8, 16, 32, 64, 16, 32, 64	82.78	84.53	81.03

Table 3. The average performance over 10 folds of the best configuration of LMPSeizNet with channels {F7-T7, F3-C3, FT9-FT10}.

	Performance		
	Avg Accuracy %	Avg Accuracy %	Avg Specificity %
Experiment 5	97.42	99.33	95.51

5.1.2. Hyperparameter Tuning

Four experiments were conducted to fine-tune different hyperparameters of the LMP-SeizNet architecture, including the filter sizes, number of filters, channel combinations, and strides with five training epochs of the optimizer for each experiment and 0.01 learning rate. First, in Experiment 1, we fixed the number of filters, the channels, and the stride and changed the filter sizes to different values in the range from 8 to 128 by increasing with a power of 2 to obtain the best performance. The results shown in Figure 4 indicate that the filter sizes T_0 = 128, T_1 = 32, T_2 = 16, and T_3 = 8 obtained the best performance, where accuracy is 90.77%, sensitivity is 92.01%, and specificity is 89.52%.

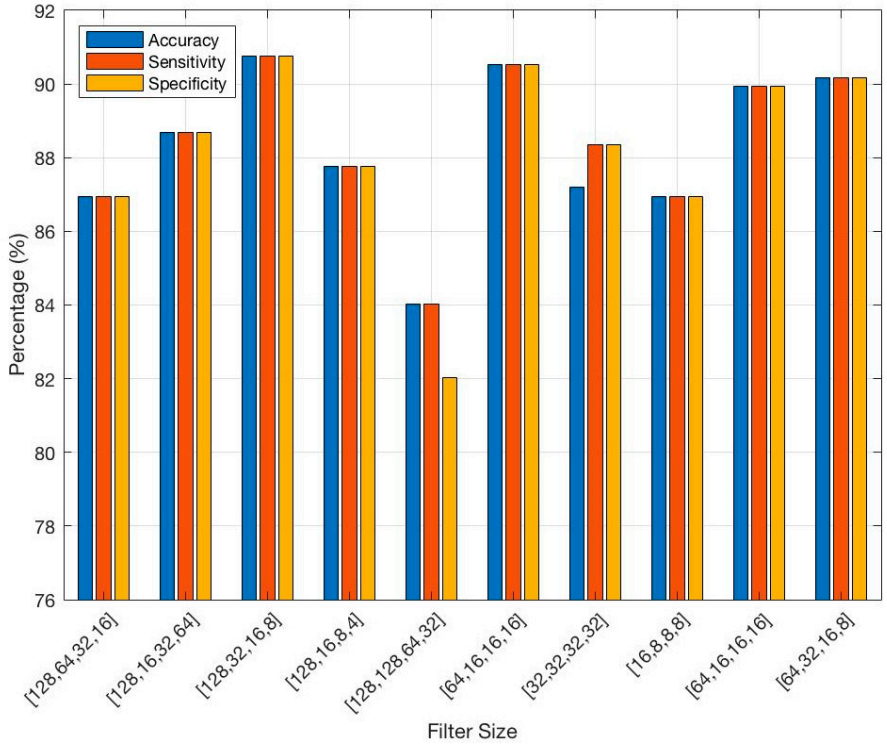

Figure 4. Results of Experiment 1 showing the effect of different choices of filter sizes [T_0,T_1, T_2, T_3]. The experiments were performed with the channels {FP1-F7, F7-T7, T7-P7} and a fixed number of filters.

Secondly, in Experiment 2, we fixed the filter sizes, channels, and strides that provided the best performance in Experiment 1 and changed the number of filters to the values in the range from 8 to 256, by increasing with a power of 2. The results demonstrated in Figure 5 reveal that the model achieved the best performance when the number of filters is 64, 32, 16, 8, 32, 16, and 8 for the TConv, TSepConv-1, TSepConv-2, TSepConv-3, SConv-1, SConv-2, and SConv-3 blocks, respectively, which obtained an accuracy equal to 90.77%, sensitivity equal to 92.01%, and specificity equal to 89.5%.

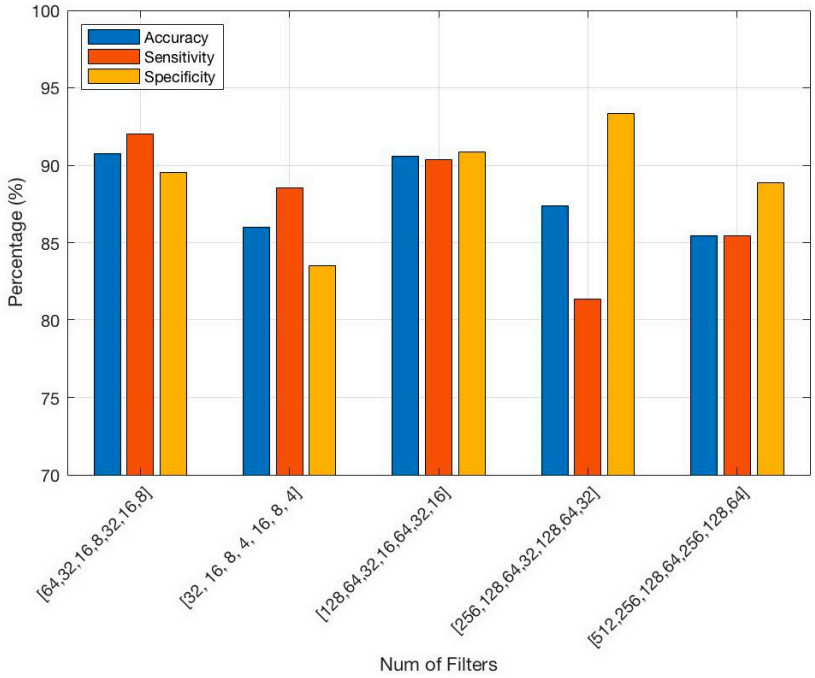

Figure 5. Results of Experiment 2 depicting the effects of varying numbers of filters [K_0, K_1, K_2, K_3, K_4, K_5, K_6] of each block [TConv, TSepConv-1, TSepConv-2, TSepConv-3, SConv-1, SConv-2, SConv-3]. The experiments were performed with the channels {FP1-F7, F7-T7, T7-P7} and fixed filter sizes.

Further, we conducted several experiments with the best configuration provided by Experiments 1 and 2 with different combinations of channels reported in refs. [35,45,46]. Precisely, the study in [46] reported that the channel combinations {F7−T7, T7−P7, F3-C7, C3−P3, P4−O2}, {F7-T7, T7-F7, C4-P4, F8-T8, T8-P8}, {F7-T7, T7-F7, F3-C3, C3-P3, P4-O2, FZ-CZ}, {FP1-F7, F7-T7, T7-P7, P7-O1, P4-O2, FZ-CZ},{P7-O1, P3-O1, C4-P4, F8-T8, T8-P8}, and {F7-T7, T7-P7, P3-O1, P4-O2, F8-T8, T8-P8} provide more than 60% successful rate. Furthermore, we conducted the experiments with the combination {F7-T7, F3-C3, FT9-FT10}, where the channels showed the highest variance, as reported in refs. [35,45,46]. The results depicted in Figure 6 show that in our case, the combination {F7-T7, F3-C3, FT9-FT10} also gives the best performance, i.e., an accuracy of 93.01%, sensitivity of 98.17%, and specificity of 87.85%. As such, we adopted this combination of channels in our experiments.

Finally, we conducted several experiments using the configuration obtained from Experiment 3 with different strides for each class to generate the EEG trials for training; each time, we changed the stride for each class with values 1, 1.5, or 2 s. The stride value equal to 2 refers to no overlapping, the stride value equal to 1.5 refers to there being 25% overlapping, and the stride value equal to 1 refers to there being 50% overlapping with the maximum number of training epochs of the optimizer to find out the best stride for each class (inter-ictal, ictal). The results illustrated in Figure 7 show that when the stride value equals 2 for each class, we obtain the best performance.

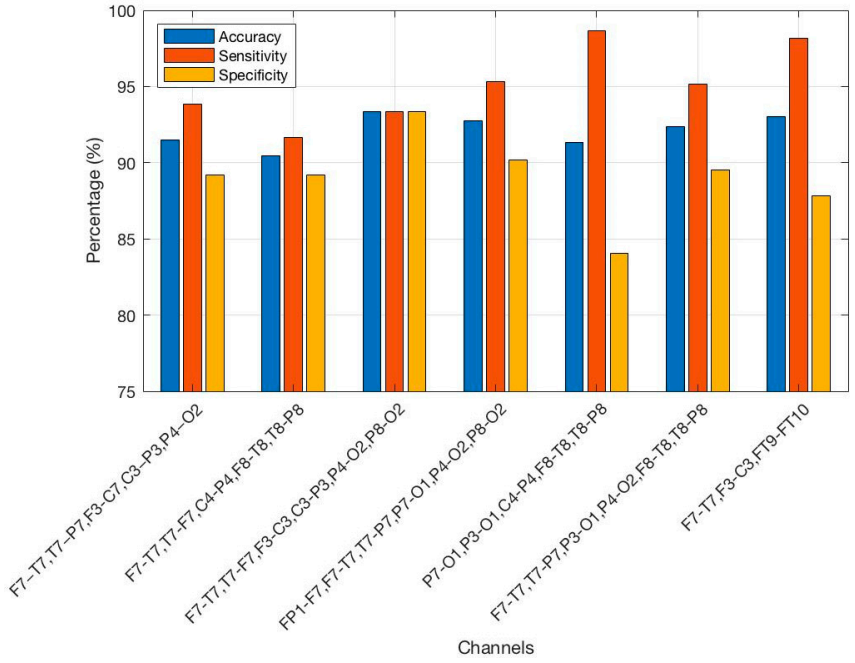

Figure 6. The results of Experiment 3 showing the effects of different combinations of channels. The experiments were performed with fixed numbers of filters and sizes.

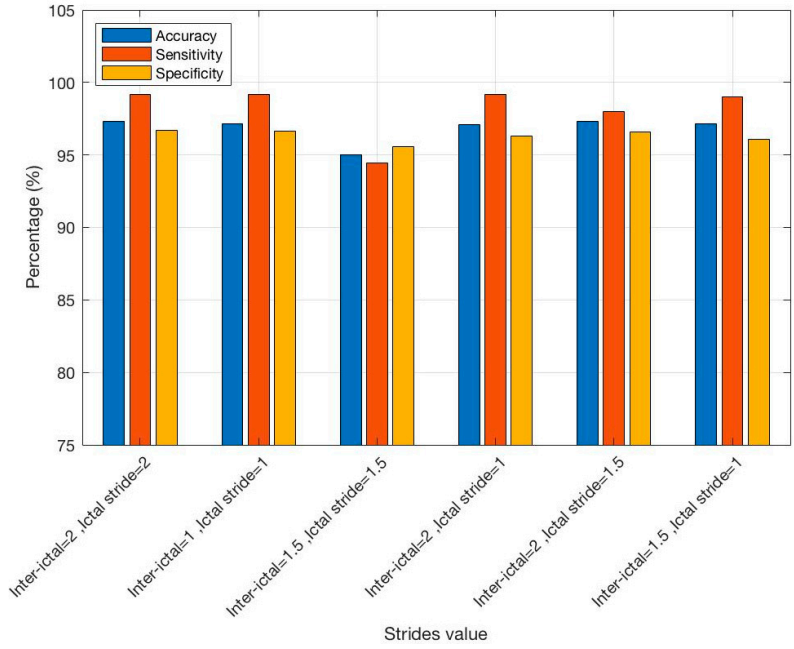

Figure 7. Results of Experiment 4 showing the effects of different stride values for sampling the EEG trials for each class. The experiments were performed with the channels {F7-T7, F3-C3, FT9-FT10} and fixed filter sizes and number of filters.

6. Experimental Results

After the ablation study, we obtained the best configuration of LMPSeizNet. Using the final model, we conducted Experiment 5 for two classes (inter-ictal and ictal) with the channels {F7-T7, F3-C3, FT9-FT10} using 10-fold cross-validation. We trained the model until we obtained the best validation accuracy for each fold and then tested it on the held-out fold as a testing set. The average performance results are shown in Table 3; we obtained an average accuracy equal to 97.42%, an average sensitivity equal to 99.33%,

and an average specificity equal to 95.51%. The results show a significant performance improvement compared to the entire performance results of the previous experiments.

6.1. Analysis of the Performance of the Proposed Method

In this section, we analyze the decision-making mechanism of the LMPSeizNet model. First, we analyze the features learned by the model using the t-SNE plot and then its decision-making with the confusion matrix in Sections 6.1.1 and 6.1.2, respectively.

6.1.1. Analysis of Features

The spatial feature representation block (ϕ^2) learns the high-level multiscale spatiotemporal features, and the prediction accuracy of the model depends on whether these features are discriminative, i.e., they have a large intra-class variation. For this purpose, we extracted features as the output of ϕ^2 and plotted them using the commonly used visualization tool t-SNE. Figure 8 shows the t-SNE plot of the extracted features of the two classes (inter-ictal and ictal). The distribution of features in the plot indicates that features belonging to the two classes have large inter-class variation, i.e., the features are discriminative and lead the model to make correct predictions in most of the cases. Though there are some misclassifications, i.e., features land on the region of the wrong class, overall, the features for the two classes form two separate clusters.

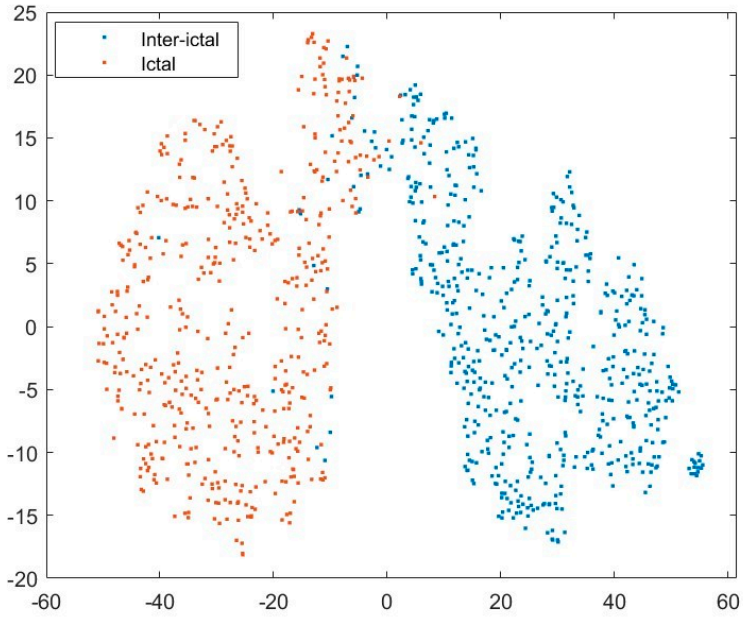

Figure 8. Visualization of the extracted features of the two classes (inter-ictal and ictal) using a t−SNE plot. The clustering of features belonging to each indicates that the two classes have a large inter-class difference, and the learned features are discriminative.

6.1.2. Analysis of Decision-Making

Generally, the confusion matrix is an efficient performance measure for classification problems and gives a deeper understanding of the internal decision-making mechanism of the classifier. It allows for visualizing and summarizing a classification algorithm's performance and permits measuring recall, precision, and accuracy. It shows the amount of confusion or uncertainty in the decisions of the model in correctly classifying the inter-ictal and ictal classes. Figure 9 shows the confusion matrix of the model for the two classes (inter-ictal and ictal). It can be noticed that 574 inter-ictal class signals are correctly classified while only 27 inter-ictal class signals are incorrectly classified as ictal class. Similarly, 597 signals' ictal classes are correctly classified, while four ictal signals are classified as inter-ictal class. This indicates that the model's level of confidence in correctly classifying the two classes is high. The small number of misclassifications is probably due to the noise in the data.

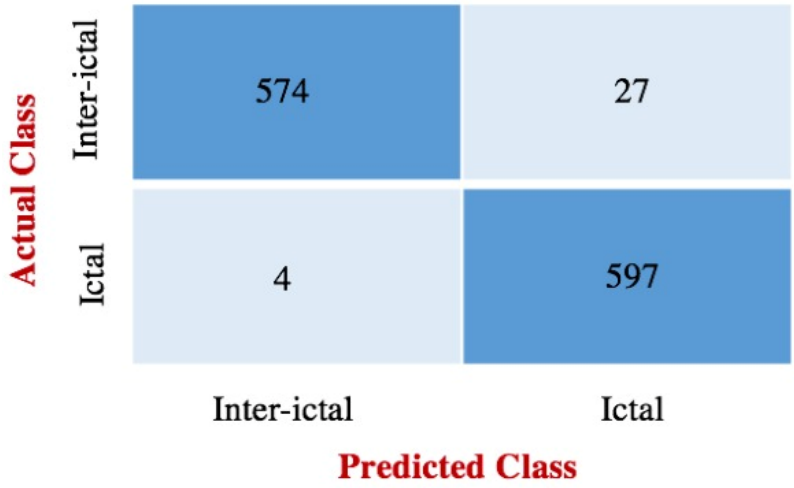

Figure 9. Confusion matrix of the best configuration of LMPSeizNet with channels {F7-T7, F3-C3, FT9-FT10}. It shows the potential of the model to classify each class.

7. Discussion

In this section, we discuss the performance of LMPSeizNet in view of the results of the experiments we performed for its validation. Firstly, we discuss the impact of its pyramid architecture. Secondly, we discuss the effects of hyperparameters of LMPSeizNet and the results obtained by the final configuration of LMPSeizNet for the two classes (inter-ictal and ictal). Finally, the performance of the model is compared with that of the state-of-the-art methods.

7.1. Results and Performance

Table 2 depicts the performance of the LMPSeizNet model with two different choices of architecture design based on the traditional and pyramid approaches. In the traditional approach, the number of filters increases as the depth of the network increases, whereas the number of filters decreases in the pyramid approach as the network goes deeper. The pyramid approach results in the reduction in the parametric complexity as well as the improvement in prediction performance; it has accuracy, sensitivity, and specificity of 86.94%, 88.52%, and 85.36%, respectively, which are better than those obtained with the traditional approach. Further, in the case of the pyramid approach, the number of learnable parameters is 18.03k, whereas it is 22.3k in the case of the traditional approach. The pyramid approach has better performance because it involves fewer parameters, and the model can be learned with the available limited amount of EEG data without overfitting. Consequently, we adopted the pyramid architecture for LMPSeizNet.

After fixing the pyramid design, we fine-tuned the various hyperparameters and performed several experiments to find the best values of filter sizes and the number of filters. The results revealed that the best filter sizes are T_0 = 128, T_1 = 32, T_2 = 16, and T_3 = 8, whereas the best numbers of filters are 64, 32, 16, 8, 32, 16, 8 for TConv, TSepConv-1, TSepConv-2, TSepConv-3, SConv-1, SConv-2, and SConv-3 blocks, respectively. Later, we used the configuration of LMPSeizNet, containing the best filter sizes and the best numbers of filters, to find the best combination of EEG channels. Keeping in view the findings in the literature, we examined different combinations of the channels, and the results revealed that the best combination of channels is {F7-T7, F3-C3, FT9-FT10}. Finally, we fixed the best combination of channels, the best filter sizes, and the number of filters to find the best value of stride for each class (inter-ictal, ictal); we found out that when there are no overlap strides, i.e., stride value equals two, we obtain the best performance. The summary of the results of each experiment for hyperparameter tuning is shown in Figures 4–7 to obtain the final configuration of LMPSeizNet. The results of the ablation experiments indicate that the different choices of the hyperparameters result in different performances of LMPSeizNet and help to find the best choices.

Finally, using the best configuration of the architecture of LMPSeizNet and the best combination of channels {F7-T7, F3-C3, FT9-FT10}, we performed experiments using 10-fold cross-validation to find out the real performance of the model across different training and test sets and to know whether the model has good generalization. The results indicate that the model shows high performance, which is comparable to one of the best state-of-the-art methods [35], and outperforms in terms of sensitivity with a shorter temporal length of EEG trials. Moreover, the number of learnable parameters of LMPSeizNet is significantly less than those of the model proposed in ref. [36]. We analyzed the features of the best configuration of LMPSeizNet and observed that the extracted features for the two classes (inter-ictal and ictal) are discriminative. Further, the confusion matrix revealed that the model is robust and makes the decision with the least confusion.

7.2. Comparison with the State-of-the-Art Methods

In this section, we compared LMPSeizNet with the state-of-the-art (SOTA) methods that addressed the same problem, i.e., non-seizure vs. seizure or inter-ictal vs. ictal, used the same evaluation protocol as we used, and evaluated using the CHB-MIT dataset. The state-of-the-art techniques used the subject-independent protocol for evaluation, with a trial length equal to two seconds. A summary of the approach of each SOTA method and its complexity in terms of the number of learnable parameters and the performance of each method in terms of accuracy, sensitivity, and specificity is given in Table 4.

Table 4. Comparison with the state-of-the-art (SOTA) methods on the CHB-MIT dataset. Each SOTA method used the same evaluation protocol as we used and addressed the same problem, i.e., non-seizure vs. seizure or inter-ictal vs. ictal. Notations: #Param—number of learnable parameters, #Sub—number of subjects, #Ch—number of channels, T.L.—the trail length.

Ref.	#Param	Method	#Sub	#Ch	TL (s)	Performance		
						Acc (%)	Sen (%)	Spe (%)
Zabihi et al. [24] (2019)	-	unonlinear dynamics and nullclines	24	23	1	95.11	91.15	95.16
Li et al. [25] (2020)	-	nonlinear modes (N.M.s) and KNN	24	4	2	98.61	98.40	99.10
Wang et al. [31] (2021)	105,538	RS-DA strategy, 1D-CNN	24	23	2	99.54	88.14	99.62
Abdelhameed et al. [36] (2021)	190,869	two-dimensional deep convolution autoencoder (2D-DCAE)	16	23	4	98.79	98.72	98.86
Rafiammal et al. [26] (2021)	-	discrete wavelet transform and Cluster-based Nearest Neighborhood machine learning algorithm	23	23	-	90.0	85.00	85.00
Lyu et al. [34] (2021)	88,813,634	GCPL	23	21	2	93.59	90.84	96.34
Zarei et al. [27] (2021)	-	discrete wavelet transform, orthogonal matching pursuit, and entropy	23	23	2	98.00	97.00	98.00
Cimr et al. [14] (2023)	15,059	CAD	24	21	2	96.99	96.89	97.06
Tripathi et al. [39] (2023)	144,000,000	superlet transform (SLT) + VGG-19	22	23	2	94.3	94.00	94.5
Abdulwahhab et al. [15] (2024)	undefined *	CNN and RNN	23	23	-	97.12	96.75	97.49
LMPSeizNet	18,024	multiscale CNN	8	3	2	97.42	99.33	95.51

* The specification of the architecture of the model is not provided; "-" means the method is based on a hand-engineered feature extraction technique.

Among them, we noted that Abdelhameed et al. [36] obtained the best performance among these studies; they achieved an accuracy equal to 98.79%, a sensitivity equal to 98.72%, and a specificity equal to 98.86%. They used 16 subjects, 23 channels, a trial length equal to four seconds, and the subject-independent protocol for evaluation. In contrast,

Rafiammal et al. [26] and Lyu et al. [34] provided the lowest performance among these studies. Both studies used 23 subjects and a subject-independent protocol for evaluation but differed in the number of channels used.

We noted that Abdelhameed et al. [36] and Zarei et al. [27] used the same evaluation protocol, the number of channels, and the number of classes. Still, they differed in the length of trials and the number of subjects, where Abdelhameed et al. [36] used a trial length equal to four and 16 subjects, while Zarei et al. [27] used a trial length equal to two and 23 subjects. However, Abdelhameed et al. [36] provided a higher performance.

Additionally, we observed that Wang et al. [31] and Li et al. [25] used the same evaluation protocols, number of subjects, and trial length, but they differed in the number of channels used, where Wang et al. [31] used 23 channels, while Li et al. [25] used 4 channels. Consequently, Li et al. [25] reported better performance on average.

When we compared the proposed method with those by Abdelhameed et al. [36] and Li et al. [25], we found that we used the same evaluation protocol as Abdelhameed et al. [36] and used the same trial length as Li et al. [25]. We noted that the proposed method outperformed both methods in terms of sensitivity; the methods by Abdelhameed et al. [36] and Li et al. [25] achieved sensitivities of 98.72% and 98.40%, respectively, whereas the proposed method achieved a sensitivity of 99.33%.

The comparison of the proposed method with that by Cimr et al. [14] indicates that LMPSeizNet uses fewer channels (i.e., 3 instead of 21) and involves slightly more learnable parameters (i.e., 18,024 vs. 15,059). However, LMPSeizNet performs better despite the slight difference in the complexity of the parameters reported by Cimr et al. [14]. There are two reasons that LMPSeizNet performs better. First, it encodes multiscale information, while Cimr et al. [14] do not use the multiscale of EEG signals; specifically, LMPSeizNet captures multiscale temporal and spatial information from an EGG trial, leading to better performance than the single scale approach by Cimr et al. [14]. Second, it does away with redundant information by focusing on salient channels and has a better capacity to learn discriminative features; it has a good trade-off between the model complexity and the amount of training data. Further, we found that Tripathi et al. [39] has a very high learnable parameter complexity, reaching 144000000, which leads it to have the third lowest performance after Rafiammal et al. [26] and Lyu et al. [34]. Finally, we compared LMPSeizNet with Abdulwahhab et al. [15]; we found that our proposed method achieved better accuracy and sensitivity with a number of subjects and channels, whereas Abdulwahhab et al. [15] did not provide the parameter complexity and the specification of the architecture of their model.

Interestingly, the proposed method achieved better sensitivity using only three channels; the proposed method decreased the computation complexity in contrast to other approaches. This is because it is based on the pyramid approach and performs multiscale analysis of EEG signals. It is important to note that sensitivity, i.e., the true positive rate, is more important for detecting epileptic seizures.

8. Conclusions

In this paper, we addressed the problem of epileptic seizure detection. Epilepsy is a chronic disease that causes a severe disturbance of neurons, causing a seizure. The rapid detection of epilepsy seizures is important to reduce the risk of seizure-related complications. The EEG technique is the most common method used for detecting epileptic seizures, and deep learning techniques employed to develop epilepsy seizure detection based on EEG signals have limitations. To overcome these limitations, we designed an efficient and lightweight multiscale convolutional neural network model (LMPSeizNet) for seizure detection on EEG signals. We evaluated the model using 10-fold cross-validation on a benchmark public domain dataset (CHB-MIT dataset), and the results showed that LMPSeizNet has better sensitivity than state-of-the-art methods despite having less parameter complexity and computational complexity. The LMPSeizNet model performs better than state-of-the-art methods because it can be trained with a limited amount of data due to

its lightweight architecture, and it analyses an EEG signal to extract spectral information using multiscale temporal convolutions. Further, extensive experiments were conducted to tune the hyperparameters of the model and to select the number of channels that play key roles in detecting ictal and inter-ictal states. We found that the channels F7-T7, F3-C3, and FT9-FT10 are effective in detecting the seizure; these channels capture the brain activations from the frontal, temporal, and central brain lobes. To determine the decision-making of LMPSeizNet that leads to its superior performance, we analyzed the features learned by the model, which indicated that it learns discriminative features, which eventually help to make correct decisions in predicting ictal and inter-ictal states. In addition, to determine how it predicts ictal and inter-ictal states, we computed the confusion matrix that revealed that the model correctly detects most cases; only a few cases are misclassified. LMPSeizNet will prove to be a helpful tool for neurologists and clinicians to detect seizures of epilepsy patients and manage their treatment. For future work, we will explore the challenging problem of detecting seizures in the inter-ictal vs. pre-ictal vs. ictal scenario and design an efficient and lightweight model for this problem.

Author Contributions: Conceptualization, A.A. and M.H.; data curation, A.A.; formal analysis, A.A. and M.A.; funding acquisition M.H.; methodology, A.A., M.A., and M.H.; project administration, M.H.; resources, M.H.; software, A.A.; supervision, M.H.; validation, A.A.; visualization, A.A. and M.A.; writing—original draft, M.A.; writing—review and editing, M.H. All authors have read and agreed to the published version of the manuscript.

Funding: This research was supported by the Researchers Supporting Project, number (RSP2024R109), King Saud University, Riyadh, Saudi Arabia.

Data Availability Statement: Public domain datasets were used for experiments.

Conflicts of Interest: The authors declare no conflicts of interest.

List of Notations

Variable	Meaning	Variable	Meaning
x	EEG epochs	K_0	one-dimensional (1D) temporal filters
C	channel	f_s	sampling rate
T	time point	$\mathcal{F}_0$	feature map of K_0
$\hat{y}$	predicted label of x	T_0, T_1, T_2, T_3	filter size
θ	learnable parameters	$K_0, K_1, K_2, K_3, K_4, K_5, K_6$	numbers of filters
$\mathcal{H}$	(LMPSeizNet) model	v_1, v_2, v_3	feature vectors
ϕ^1	the multiscale temporal feature representation	p	posterior probabilities vector
ϕ^2	the spatial feature representation	$\hat{\theta}$	minimal loss
ϕ^3	the classifier	TP	number of true positives
Acc	accuracy rate	TN	number of true negatives
Sen	sensitivity rate (true positive rate)	FP	number of false positives
Spe	specificity rate (true negative rate)	FN	number of false negatives

References

1. Ghassemi, N.; Shoeibi, A.; Rouhani, M.; Hosseini-Nejad, H. Epileptic seizures detection in EEG signals using TQWT and ensemble learning. In Proceedings of the 2019 9th International conference on computer and knowledge engineering (ICCKE), Mashhad, Iran, 24–25 October 2019; IEEE: Piscataway, NJ, USA, 2019; pp. 403–408.
2. Ansari, A.Q.; Sharma, P.; Tripathi, M. Automatic seizure detection using neutrosophic classifier. *Phys. Eng. Sci. Med.* **2020**, *43*, 1019–1028. [CrossRef]
3. Bhattacharyya, A.; Pachori, R.B.; Upadhyay, A.; Acharya, U.R. Tunable-Q wavelet transform based multiscale entropy measure for automated classification of epileptic EEG signals. *Appl. Sci.* **2017**, *7*, 385. [CrossRef]
4. Xu, G.; Ren, T.; Chen, Y.; Che, W. A one-dimensional CNN-LSTM model for epileptic seizure recognition using EEG signal analysis. *Front. Neurosci.* **2020**, *14*, 578126. [CrossRef]
5. Shoeibi, A.; Khodatars, M.; Ghassemi, N.; Jafari, M.; Moridian, P.; Alizadehsani, R.; Panahiazar, M.; Khozeimeh, F.; Zare, A.; Hosseini-Nejad, H.; et al. Epileptic seizures detection using deep learning techniques: A review. *Int. J. Environ. Res. Public Health* **2021**, *18*, 5780. [CrossRef]

6. Kulaseharan, S.; Aminpour, A.; Ebrahimi, M.; Widjaja, E. Identifying lesions in paediatric epilepsy using morphometric and textural analysis of magnetic resonance images. *NeuroImage Clin.* **2019**, *21*, 101663. [CrossRef]
7. Zazzaro, G.; Cuomo, S.; Martone, A.; Montaquila, R.V.; Toraldo, G.; Pavone, L. EEG signal analysis for epileptic seizures detection by applying data mining techniques. *Internet Things* **2021**, *14*, 100048. [CrossRef]
8. van Klink, N.; Mooij, A.; Huiskamp, G.; Ferrier, C.; Braun, K.; Hillebrand, A.; Zijlmans, M. Simultaneous MEG and EEG to detect ripples in people with focal epilepsy. *Clin. Neurophysiol.* **2019**, *130*, 1175–1183. [CrossRef]
9. Kim, T.; Nguyen, P.; Pham, N.; Bui, N.; Truong, H.; Ha, S.; Vu, T. Epileptic seizure detection and experimental treatment: A review. *Front. Neurol.* **2020**, *11*, 701. [CrossRef]
10. Rizal, A.; Priharti, W.; Hadiyoso, S. Seizure Detection in Epileptic EEG Using Short-Time Fourier Transform and Support Vector Machine. *Int. J. Online Biomed. Eng.* **2021**, *17*, 65. [CrossRef]
11. Subasi, A.; Kevric, J.; Abdullah Canbaz, M. Epileptic seizure detection using hybrid machine learning methods. *Neural Comput. Appl.* **2019**, *31*, 317–325. [CrossRef]
12. Wang, X.; Gong, G.; Li, N. Automated recognition of epileptic EEG states using a combination of symlet wavelet processing, gradient boosting machine, and grid search optimizer. *Sensors* **2019**, *19*, 219. [CrossRef] [PubMed]
13. Lotte, F.; Bougrain, L.; Clerc, M. Electroencephalography (EEG)-based brain-computer interfaces. *Wiley Encycl. Electr. Electron. Eng.* **2015**, 44.
14. Cimr, D.; Fujita, H.; Tomaskova, H.; Cimler, R.; Selamat, A. Automatic seizure detection by convolutional neural networks with computational complexity analysis. *Comput. Methods Programs Biomed.* **2023**, *229*, 107277. [CrossRef] [PubMed]
15. Abdulwahhab, A.H.; Abdulaal, A.H.; Al-Ghrairi, A.H.T.; Mohammed, A.A.; Valizadeh, M. Detection of epileptic seizure using EEG signals analysis based on deep learning techniques. *Chaos Solitons Fractals* **2024**, *181*, 114700. [CrossRef]
16. Ko, W.; Jeon, E.; Jeong, S.; Suk, H.-I. Multi-scale neural network for EEG representation learning in BCI. *IEEE Comput. Intell. Mag.* **2021**, *16*, 31–45. [CrossRef]
17. Ullah, I.; Hussain, M.; Aboalsamh, H. An automated system for epilepsy detection using EEG brain signals based on deep learning approach. *Expert Syst. Appl.* **2018**, *107*, 61–71. [CrossRef]
18. Sunaryono, D.; Sarno, R.; Siswantoro, J. Gradient boosting machines fusion for automatic epilepsy detection from EEG signals based on wavelet features. *J. King Saud Univ.-Comput. Inf. Sci.* **2022**, *34*, 9591–9607. [CrossRef]
19. Anuragi, A.; Sisodia, D.S.; Pachori, R.B. Epileptic-seizure classification using phase-space representation of FBSE-EWT based EEG sub-band signals and ensemble learners. *Biomed. Signal Process. Control* **2022**, *71*, 103138. [CrossRef]
20. Sharma, M.; Patel, S.; Acharya, U.R. Automated detection of abnormal EEG signals using localized wavelet filter banks. *Pattern Recognit. Lett.* **2020**, *133*, 188–194. [CrossRef]
21. Go, A.; Bhayani, R.; Huang, L. *Twitter Sentiment Classification Using Distant Supervision*; Stanford University: Stanford, CA, USA, 2009; Volume 1, p. 2009.
22. Davidson, S.; McCallan, N.; Ng, K.Y.; Biglarbeigi, P.; Finlay, D.; Lan, B.L.; McLaughlin, J. Epileptic seizure classification using combined labels and a genetic algorithm. In Proceedings of the 2022 IEEE 21st Mediterranean Electrotechnical Conference (MELECON), Palermo, Italy, 14–16 June 2022; IEEE: Piscataway, NJ, USA, 2022; pp. 430–435.
23. Zinkus, M.; Jois, T.M.; Green, M. Data security on mobile devices: Current state of the art, open problems, and proposed solutions. *arXiv* **2021**, arXiv:2105.12613.
24. Zabihi, M.; Kiranyaz, S.; Jäntti, V.; Lipping, T.; Gabbouj, M. Patient-specific seizure detection using nonlinear dynamics and nullclines. *IEEE J. Biomed. Health Inform.* **2019**, *24*, 543–555. [CrossRef]
25. Li, M.; Sun, X.; Chen, W. Patient-specific seizure detection method using nonlinear mode decomposition for long-term EEG signals. *Med. Biol. Eng. Comput.* **2020**, *58*, 3075–3088. [CrossRef]
26. Syed Rafiammal, S.; Najumnissa Jamal, D.; Kaja Mohideen, S. Detection of epilepsy seizure in adults using discrete wavelet transform and cluster nearest neighborhood classifier. *Iran. J. Sci. Technol. Trans. Electr. Eng.* **2021**, *45*, 1103–1115. [CrossRef]
27. Zarei, A.; Asl, B.M. Automatic seizure detection using orthogonal matching pursuit, discrete wavelet transform, and entropy based features of EEG signals. *Comput. Biol. Med.* **2021**, *131*, 104250. [CrossRef] [PubMed]
28. Gupta, S.; Meena, J.; Gupta, O. Neural network based epileptic EEG detection and classification. *arXiv* **2020**, arXiv:2111.03268. [CrossRef]
29. Jia, G.; Lam, H.-K.; Althoefer, K. Variable weight algorithm for convolutional neural networks and its applications to classification of seizure phases and types. *Pattern Recognit.* **2022**, *121*, 108226. [CrossRef]
30. Liu, Y.; Sivathamboo, S.; Goodin, P.; Bonnington, P.; Kwan, P.; Kuhlmann, L.; O'Brien, T.; Perucca, P.; Ge, Z. Epileptic seizure detection using convolutional neural network: A multi-biosignal study. In Proceedings of the Australasian Computer Science Week Multiconference, Melbourne, Australia, 4–6 February 2020; pp. 1–8.
31. Wang, X.; Wang, X.; Liu, W.; Chang, Z.; Kärkkäinen, T.; Cong, F. One dimensional convolutional neural networks for seizure onset detection using long-term scalp and intracranial EEG. *Neurocomputing* **2021**, *459*, 212–222. [CrossRef]
32. Liu, Y.; Huang, Y.-X.; Zhang, X.; Qi, W.; Guo, J.; Hu, Y.; Zhang, L.; Su, H. Deep C-LSTM neural network for epileptic seizure and tumor detection using high-dimension EEG signals. *IEEE Access* **2020**, *8*, 37495–37504. [CrossRef]
33. Takahashi, H.; Emami, A.; Shinozaki, T.; Kunii, N.; Matsuo, T.; Kawai, K. Convolutional neural network with autoencoder-assisted multiclass labelling for seizure detection based on scalp electroencephalography. *Comput. Biol. Med.* **2020**, *125*, 104016. [CrossRef] [PubMed]

34. Lyu, C.; Chen, Y.; Chen, Z.; Liu, Y.; Wang, Z. Automatic epilepsy detection based on generalized convolutional prototype learning. *Measurement* **2021**, *184*, 109954. [CrossRef]
35. Ein Shoka, A.A.; Alkinani, M.H.; El-Sherbeny, A.; El-Sayed, A.; Dessouky, M.M. Automated seizure diagnosis system based on feature extraction and channel selection using EEG signals. *Brain Inform.* **2021**, *8*, 1. [CrossRef] [PubMed]
36. Abdelhameed, A.; Bayoumi, M. A deep learning approach for automatic seizure detection in children with epilepsy. *Front. Comput. Neurosci.* **2021**, *15*, 650050. [CrossRef]
37. Escorcia-Gutierrez, J.; Beleno, K.; Jimenez-Cabas, J.; Elhoseny, M.; Alshehri, M.D.; Selim, M.M. An automated deep learning enabled brain signal classification for epileptic seizure detection on complex measurement systems. *Measurement* **2022**, *196*, 111226. [CrossRef]
38. Mekruksavanich, S.; Jitpattanakul, A. Effective Detection of Epileptic Seizures through EEG Signals Using Deep Learning Approaches. *Mach. Learn. Knowl. Extr.* **2023**, *5*, 1937–1952. [CrossRef]
39. Tripathi, P.M.; Kumar, A.; Kumar, M.; Komaragiri, R.S. Automatic seizure detection and classification using super-resolution superlet transform and deep neural network-A preprocessing-less method. *Comput. Methods Programs Biomed.* **2023**, *240*, 107680. [CrossRef]
40. Shoeb, A.H. *Application of Machine Learning to Epileptic Seizure Onset Detection and Treatment*; Massachusetts Institute of Technology: Cambridge, MA, USA, 2009.
41. Guttag, J. CHB-MIT Scalp EEG Databas. 2010. Available online: https://physionet.org/content/chbmit/1.0.0/ (accessed on 1 March 2023).
42. Jana, G.C.; Sharma, R.; Agrawal, A. A 1D-CNN-spectrogram based approach for seizure detection from EEG signal. *Procedia Comput. Sci.* **2020**, *167*, 403–412. [CrossRef]
43. Gao, Y.; Gao, B.; Chen, Q.; Liu, J.; Zhang, Y. Deep convolutional neural network-based epileptic electroencephalogram (EEG) signal classification. *Front. Neurol.* **2020**, *11*, 525678. [CrossRef]
44. Aslan, M.F.; Unlersen, M.F.; Sabanci, K.; Durdu, A. CNN-based transfer learning–BiLSTM network: A novel approach for COVID-19 infection detection. *Appl. Soft Comput.* **2021**, *98*, 106912. [CrossRef]
45. Bongiorni, L.; Balbinot, A. Evaluation of recurrent neural networks as epileptic seizure predictor. *Array* **2020**, *8*, 100038. [CrossRef]
46. Chang, N.-F.; Chen, T.-C.; Chiang, C.-Y.; Chen, L.-G. Channel selection for epilepsy seizure prediction method based on machine learning. In Proceedings of the 2012 Annual International Conference of the IEEE Engineering in Medicine and Biology Society, San Diego, CA, USA, 28 August–1 September 2012; IEEE: Piscataway, NJ, USA, 2012; pp. 5162–5165.

Disclaimer/Publisher's Note: The statements, opinions and data contained in all publications are solely those of the individual author(s) and contributor(s) and not of MDPI and/or the editor(s). MDPI and/or the editor(s) disclaim responsibility for any injury to people or property resulting from any ideas, methods, instructions or products referred to in the content.